

Integral spinors, Apollonian disk packings, and Descartes groups

Jerzy Kocik

Department of Mathematics, Southern Illinois University, Carbondale, IL62901
jkocik@siu.edu

Abstract

We show that every irreducible integral Apollonian packing can be set in the Euclidean space so that all of its tangency spinors and all reduced coordinates and co-curvatures are integral. As a byproduct, we prove that in any integral Descartes configuration, the sum of the curvatures of two adjacent disks can be written as a sum of two squares. Descartes groups are defined, and an interesting occurrence of the Fibonacci sequence is found.

Keywords: Descartes theorem, Apollonian disk packing, tangency spinors, Descartes group, sum of squares theorem, Fibonacci sequence.

MSC: 52C26, 28A80, 51M15, 11A99.

1. Introduction

Apollonian disk packings, the examples of which are presented in Figure 1 and 2, convey a rich number-theoretic content. To start with, there exist “integral packings” where the curvatures of the disks (the numbers in the figures) are all integers. There are infinitely many such packings. Curvatures are not the only magnitudes associated with the disks. There are also disk symbols – related to the disks positions – and the tangency spinors. The main question is if the integrality of these quantities (especially the spinors) is possible.

Section 3 clarifies these terms and introduces a few new convenient concepts.

Section 4 presents the main result: the proof that indeed every Apollonian packing may be located in the plane so that such a “hyper-integrality” is attained.

Section 5 proves some properties of the concepts used in the proof.

Section 6 discusses an interesting order of the Apollonian disk packings that emerged in due process, including an intriguing exceptional case of a “Fibonacci” family.

Finally, Section 7 discusses the group-theoretic aspect of these concepts. In particular, we define the Descartes group and kaleidoscope group, and their action on triples and quadruples of tangent disks.

We start with an associated minor, yet intriguing, observation that seem to have been missed, namely, that the sum of the curvatures of two adjacent disks in such packings can always be presented as a sum of two squares, as explained in Section 2. Proving this fact directly may be a rather challenging task, while we will procure it as a corollary to the main theorem.

This paper is companion to [10], where the integral Apollonian packings are derived from spinors only.

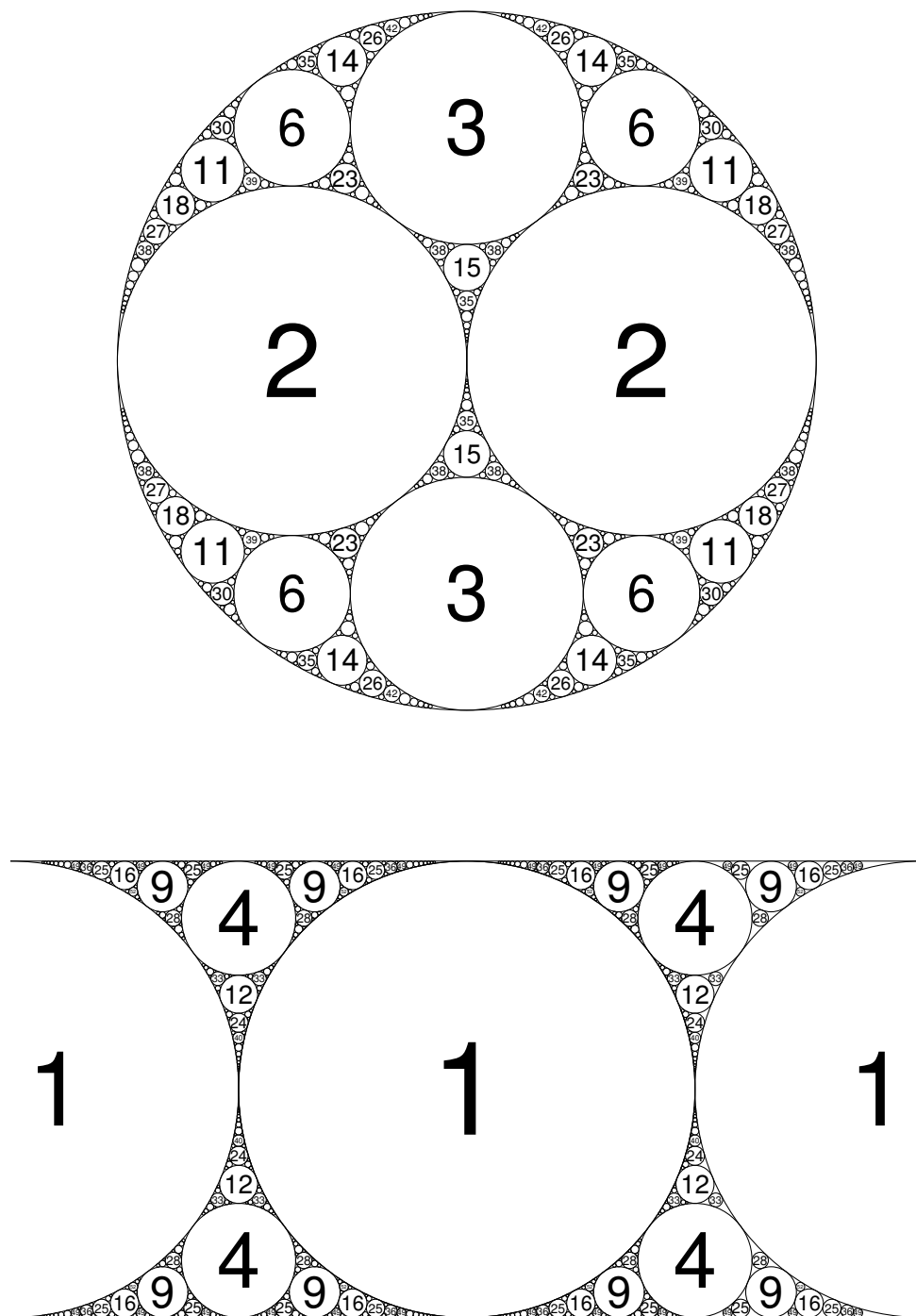


FIGURE 1: At the top: Apollonian Window. At the bottom: Apollonian Belt

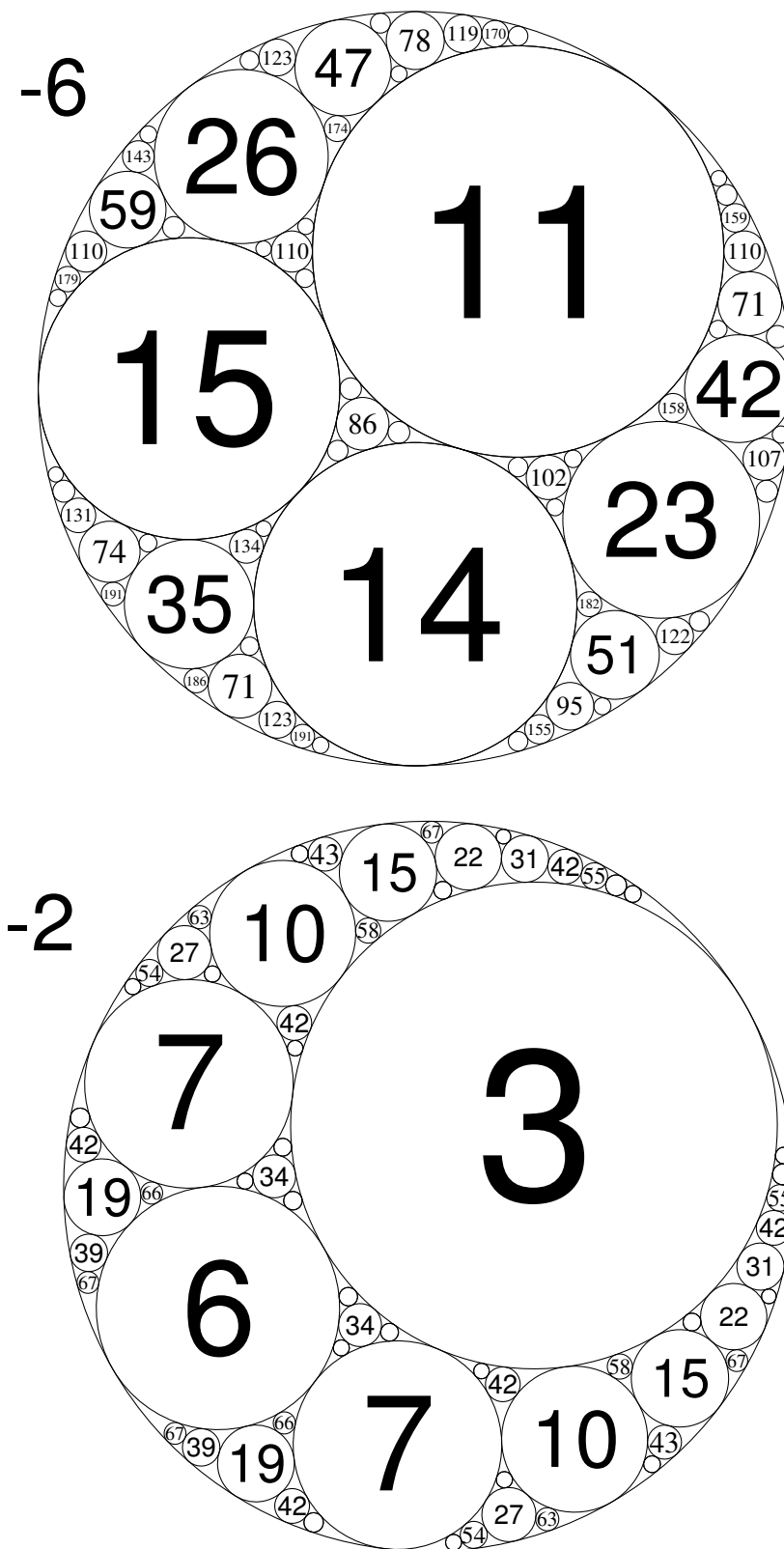


FIGURE 2: Two other examples of irreducible integral packings. The curvature of the exterior disk at the top is -6 , at the bottom: -2 .

2. Curious sums

Irreducible integral Apollonian disk packings (see Figures 1 and 2 for examples), have many interesting number-theoretic properties, many of which have been analyzed in various contexts [12, 2, 16].

But the following feature seems to be overlooked: the sum of two curvatures of any two disks in contact is always a number that can be represented as a sum of squares. Here are examples read off from the Apollonian Window (Fig. 1):

$$-1 + 6 = 5 = 1^2 + 2^2 \quad 3 + 6 = 9 = 0^2 + 3^2 \quad 6 + 23 = 29 = 5^2 + 2^2$$

We may reduce this statement to the Descartes configurations, i.e., configurations of four mutually tangent disks, and pose it as a purely number-theoretic statement, without reference to geometry:

Proposition 2.1. If a quadruple of non-negative integers a, b, c, d is primitive, i.e., such that $\gcd(a, b, c, d) = 1$, and satisfies the quadratic equation:

$$(a + b + c + d)^2 = 2(a^2 + b^2 + c^2 + d^2) \quad (2.1)$$

then the sum of any two is a sum of two squares:

$$a + b = p^2 + q^2 \quad (2.2)$$

for some $p, q \in \mathbf{Z}$.

In principle, the property (2.2) should be provable in purely number-theoretic manner from condition (2.1). We leave it as an interesting challenge. A verification of this property will arise as a byproduct of the main result in these notes, see Corollary 4.2. The condition of non-negativity may be relaxed to at most one of a, b, c, d being negative.

Remark on the sums of squares: Sums of squares were studied by Euler. Here are the cases up to 100: 1, 2, 4, 5, 8, 9, 10, 13, 16, 17, 18, 20, 25, 26, 29, 32, 34, 36, 37, 40, 41, 45, 49, 50, 52, 53, 58, 61, 64, 65, 68, 72, 73, 74, 80, 81, 82, 85, 89, 90, 97, 98, 100. [43 out of 100]. None of the remaining 57 numbers may be found in any integral packings. The frequency of numbers that can be found is decreasing with the magnitude, as described by Landau's theorem [13, 14]. The density of such numbers among integers drops with n

$$\frac{|S(n)|}{n} \approx \frac{b}{\sqrt{\ln n}} \quad \text{for large } n,$$

where $b = 0.764223\dots$ is known as the Landau-Ramanujan constant and $S(n)$ denotes the set of all integers not exceeding n that are sums of two squares. Only one-fifth of the first million numbers can be represented as the sum of squares, only one-sixth in the first billion, and only one in seven in the first trillion.

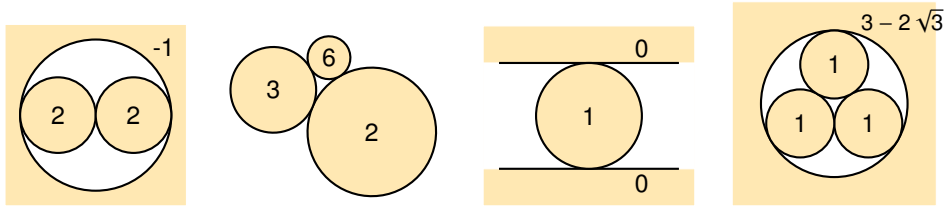


FIGURE 3: Examples of tricycles. The first three are proper integral. the last, (1,1,1), is not.

3. Terminology and basic facts

- A disk and its curvature will usually be denoted by the same (capital) letter, like A , B , C , etc. The disk that extends outside the circle bounding it has a negative curvature. A **disk symbol** of a disk A is fraction-like entity

$$\mathbf{A} = \frac{\dot{x}, \dot{y}}{A} \quad (3.1)$$

The meaning (decoding) of the symbol of disk A is

$$\text{the center} = (x, y) = \left(\frac{\dot{x}}{A}, \frac{\dot{y}}{A} \right), \quad \text{radius} = \frac{1}{A}$$

The symbol may be extended to the vector \mathbf{A} in Minkowski space [3, 4] that will be presented in two ways:

$$\frac{\dot{x}, \dot{y}}{A} \mapsto \frac{\dot{x}, \dot{y}}{A, A^c} = \begin{bmatrix} \dot{x} \\ \dot{y} \\ A \\ A^c \end{bmatrix}, \quad (3.2)$$

where $\dot{x} = x/r = Ax$, $\dot{y} = y/r = Ay$ will be called **reduced coordinates**, the curvature $A = 1/r$ is the reciprocal radius (possibly negative if the disk extends outside a circle), and A^c , which coincides with the curvature of the disk under inversion in the unit circle, will be called **co-curvature** of the disk (we follow the terminology of [3]). The inner product in the Minkowski space corresponds to the quadratic form $Q = -\dot{x}^2 - \dot{y}^2 + AA^c$ and can be expressed by Gram matrix G :

$$G = \begin{bmatrix} -1 & 0 & 0 & 0 \\ 0 & -1 & 0 & 0 \\ 0 & 0 & 0 & 1/2 \\ 0 & 0 & 1/2 & 0 \end{bmatrix} \quad (3.3)$$

By a change of basis we get coordinates that are standard in describing space-time in physics (index “ST” may stand for both “standard” and “space-time”):

$$\begin{bmatrix} \dot{x} \\ \dot{y} \\ z \\ t \end{bmatrix}_{\text{ST}} = \begin{bmatrix} \dot{x} \\ \dot{y} \\ (A - A^c)/2 \\ (A + A^c)/2 \end{bmatrix}_{\text{ST}} \quad G_{\text{ST}} = \begin{bmatrix} -1 & 0 & 0 & 0 \\ 0 & -1 & 0 & 0 \\ 0 & 0 & -1 & 0 \\ 0 & 0 & 0 & 1 \end{bmatrix} \quad (3.4)$$

- An arrangement of disks is **integral** if the curvatures of the disks are integers. It is called **primitive** if additionally their greatest common divisor is 1. It is **superintegral** if the symbols (3.2) are integral and **hyperintegral** if also tangency spinors (see below) are integral.
- A **Descartes configuration** is a system of four mutually tangent disks. Descartes' formula relates the curvatures:

$$(A + B + C + D)^2 = 2(A^2 + B^2 + C^2 + D^2) \quad (3.5)$$

It follows [15] that, given A, B, C , one has two solutions for D :

$$D_{1,2} = A + B + C \pm 2\sqrt{AB + BC + CA} \quad (3.6)$$

with D_1 and D_2 called Descartes **conjugates** through A, B, C .

- A **tricycle** is the system of three mutually tangent disks. A **Descartes completion** of a tricycle is the Descartes configuration containing the tricycle as a subset (one of the two possible). A tricycle is **proper** if it is primitive and its Descartes completion is integral. Triple $(1, 1, 1)$ is integral yet not proper, since the fourth disk of its Descartes completion is

$$D = 1 + 1 + 1 \pm \sqrt{1 \cdot 1 + 1 \cdot 1 + 1 \cdot 1} = 3 \pm 2\sqrt{3},$$

which is evidently non-rational. We also define the weight of the tricycle t of curvatures (A, B, C) as

$$w(t) = A + B + C$$

Note that any tricycle has positive weight. The smallest possible weight of an integral tricycle is 1, assumed by one presented in Figure 3.

- The **Apollonian completion** of a tricycle or Descartes configuration is the unique Apollonian disk packing containing it.
- Apollonian completion of any integral (primitive) Descartes configuration is an integral (primitive) Apollonian disk packing. This is true also for **proper** (primitive) tricycles.
- A **tangency spinor** is defined for any two tangent disks A and B as follows. Consider the plane as the complex plane and the vector joining the center of A to the center of B as a complex number $z \in \mathbb{C}$. The tangency spinor oriented from A to B is defined up to the sign as

$$\text{spin}(A, B) = \pm \sqrt{\frac{z}{r_A r_B}} \quad (3.7)$$

where $r_A = 1$ and r_B are radii of the disks (possibly negative). We will view it interchangeably either as a complex number or as a vector in \mathbb{R}^2 :

$$u = \text{spin}(A, B) = m + ni = \begin{bmatrix} m \\ n \end{bmatrix}, \quad u^\dagger = \text{spin}(B, A) = -n + mi = \begin{bmatrix} -n \\ m \end{bmatrix} \quad (3.8)$$

(both up to a sign). Using circle symbols and following our convention of using the same symbol for a disk and its curvature, one may easily derive the formula

$$u^2 = \begin{vmatrix} A & B \\ \dot{x}_A & \dot{x}_B \end{vmatrix} + \begin{vmatrix} A & B \\ \dot{y}_A & \dot{y}_B \end{vmatrix} i$$

Or, equivalently, denoting

$$\Delta_{AB} = \begin{vmatrix} A & B \\ \dot{x}_A & \dot{x}_B \end{vmatrix} \quad s = \text{sign of } \begin{pmatrix} \begin{vmatrix} A & B \\ \dot{y}_A & \dot{y}_B \end{vmatrix} \end{pmatrix}$$

the spinor oriented from A to B can be calculated as

$$\text{spin}(A, B) = \sqrt{\frac{A+B+\Delta_{AB}}{2}} + s \cdot \sqrt{\frac{A+B-\Delta_{AB}}{2}} i \quad (3.9)$$

In any Apollonian disk packing, if any two adjacent spinors, i.e., spinors $\text{spin}(A, B)$ and $\text{spin}(A, C)$ for some tricycle in the packing, are integral then all spinors in the packing are integral. For more see [8, 7, 11, 10].

4. Hyper-integrality — the main result

Here is the main theorem:

Theorem 4.1. For every irreducible integral Descartes configuration (and consequently Apollonian disk packing) there exists a positioning in the Euclidean plane such that the following are integral:

1. all entries of the disk symbols: curvatures (by assumption), co-curvatures, and reduced coordinates A, A^c, \dot{x}, \dot{y} ;
2. tangency spinors $u = [m, n]^T$;
3. disk vectors in the Minkowski space in the standard space-time coordinates, i.e., z and t of (3.4).

Proof. Here is the outline of the proof, the details of which are clarified in the following section. Start with an integral irreducible packing, understood as a structured set of curvatures (positions are not necessarily integral, or not even known). Pick an arbitrary tricycle (or Descartes configuration) in it, A, B, C . For convenience, assume an increasing order $A \leq B \leq C$. Perform a chain of the transformations $(A, B, C) \mapsto (A', B', C') = T(A, B, C)$ defined as a map

$$T(A, B, C) = \begin{cases} (-A, B+2A, C+2A) & \text{if } A < 0 \quad (*) \\ (A, B, A+B+C-2\sqrt{AB+BC+CA}) & \text{otherwise} \quad (**) \end{cases} \quad (4.1)$$

followed by ordering the resulting triple to $A' \leq B' \leq C'$. Map (*) will be called a “descending self-inversion” and is due to an inversion in the circle that bounds a disk of negative curvature A . Map (**) will be called the “descending Descartes move” and is due to replacement of the smallest disk by the greater from the two that would complete the triple to Descartes configuration. Both are described in detail in subsequent material.

In both cases the weight is strictly decreasing,

$$w(A', B', C') < w(A, B, C),$$

and preserves integrality of all ingredients (symbols and spinors). Hence, the iteration of map T must end up with the lowest-weight triple $(0, 0, 1)$. Now, this

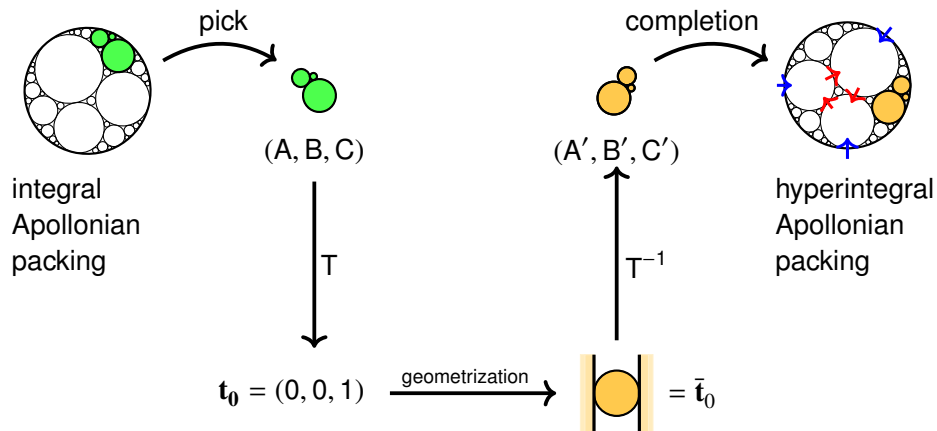


FIGURE 5: The idea of the proof. Symbol T stands for the composition of the descending transformations, and T^{-1} for its inverse. Triple (A, B, C) are curvatures of an arbitrary selection of a tricycle, and (A', B', C') the tricycle with symbols and spinors being integral.

particular triple may be realized geometrically as shown in Figure 4 below, with all entries of the symbol and of the tangency spinors being integral.

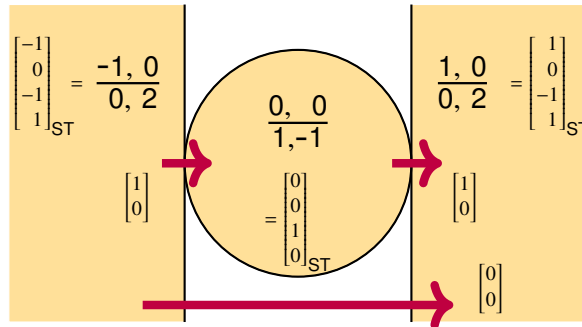


FIGURE 4: The lowest-weight base tricycle \bar{t}_0 in the integral position.

Applying the inverse of the chain of the transformation to this tricycle will recreate the original tricycle, but now in the integral position. The completion of this tricycle to the Apollonian packing will result in the hyper-integral Apollonian packing with the curvatures that of the original packing. The details are clarified in the subsequent section. \square

The puzzling property of Proposition 2.1 receives an indirect proof:

Corollary 4.2. Since the tangency spinors in any integral primitive Apollonian packing may be made integral, and its norm squared is the sum of the corresponding disks, Proposition 2.1 holds.

Corollary 4.3. In an irreducible Apollonian disk packing, the curvatures and co-curvatures of each disk share the parity, i.e., $2|(A + A^c)$. This due to the fact that t and z in the standard basis (3.4) admit integrality too.

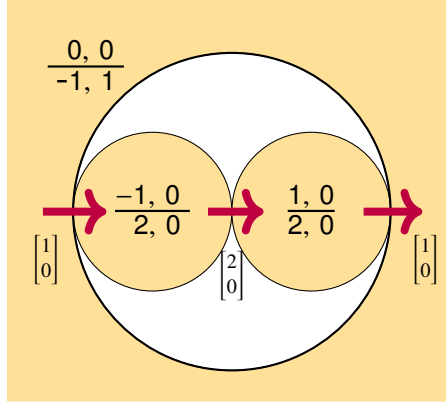


FIGURE 6: A tricycle generating the Apollonian Window, the image of inversion of which is the lowest weight tricycle, see Fig. 4.

Remark 4.4. The symbols and spinors of the base tricycle shown in Figure 4 are slightly challenging due to the presence of half-plane disks. Hence, it is convenient to start with a clear tricycle shown in Figure 6 (known from the Apollonian Window) and apply inversion through the main circle $(0, 0)/(-1, 1)$.

5. Tricycle walks

In this section we describe the two types of moves of (4.1) in the space of tricycles.

5.1. Tricycle self-inversions

Every disk X defines a circle ∂X , its boundary. As such, it defines an inversion through this circle, $\text{Inv}_{\partial X}$. It can be shown that inversion of disk C in circle K corresponds in the Minkowski space to reflection of vector \mathbf{C} in the hyper-plane \mathbf{K}^\perp orthogonal to vector \mathbf{K} . The well-known formula for such reflection in the Euclidean or pseudo-Euclidean space is

$$\mathbf{C} \mapsto \text{Inv}_K(\mathbf{C}) = \mathbf{C} - 2 \frac{\langle \mathbf{K}, \mathbf{C} \rangle}{\langle \mathbf{K}, \mathbf{K} \rangle} \mathbf{K}$$

Since the norm squared of disks is (-1) , the formula for disks reduces to

$$\mathbf{C} \mapsto \text{Inv}_K(\mathbf{C}) = \mathbf{C} + 2\langle \mathbf{K}, \mathbf{C} \rangle \mathbf{K}$$

In addition, if disk C and K are tangent, the formula reduces further to

$$\text{Inv}_K : \mathbf{C} \mapsto \mathbf{C} + 2\mathbf{K} \quad (5.1)$$

In the symbol-like notation:

$$\frac{\dot{x}_C, \dot{y}_C}{C, C^c} \mapsto \frac{\dot{x}_C + 2\dot{x}_K, \dot{y}_C + 2\dot{y}_K}{C + 2K, C^c + 2K^c} \quad (5.2)$$

If both disks are integral, so is the image C' .

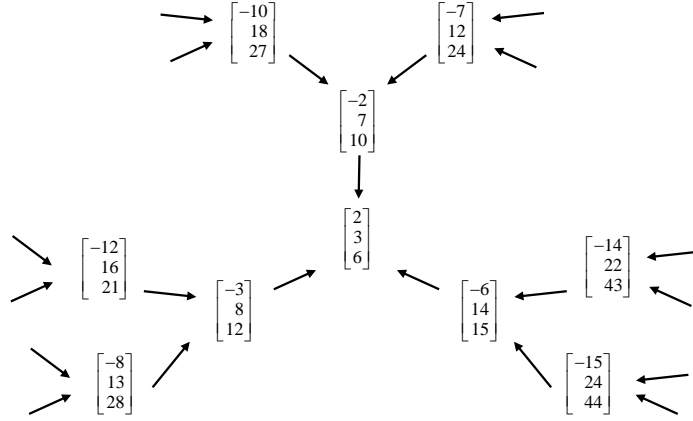


FIGURE 7: The digraph of tricycles with the relation defined by descending self-inversion. Note that $[2, 3, 6]$ is the terminal vertex.

Definition 5.1. Self-inversion of a tricycle (A, B, C) is an inversion through one of its circles ∂A , ∂B , or ∂C . A **descending self-inversion** is defined as the inversion through the circle bounding the disk of negative curvature if such exists among (A, B, C) . Otherwise, it is not defined.

Following (5.2), the curvatures of a tricycle are transformed by self-inversion through ∂A as follows

$$(A, B, C) \xrightarrow{\text{Inv}_{\partial A}} (-A, B + 2A, C + 2A) \tag{5.3}$$

Assuming the first disk being negative, the above describes the descending self-inversion.

Remark: The self-inversive moves define a 3-valent graph, and the *descending* self-inversive move defines a digraph based on the same graph.

Proposition 5.2. Under a descending self-inversive transformation, the weight function is strictly decreasing.

Proof. A simple verification: denoting $\mathbf{t} = (A, B, C)$ and $\mathbf{t}' = T(\mathbf{t}) = (A', B', C')$, we have

$$w(\mathbf{t}') = A' + B' + C' = (-A) + (B+2A) + (C+2A) = w(T(\mathbf{t})) + 2A$$

Since descending self-inversion is defined for $A < 0$, the claim holds. □

Corollary 5.3. Eq. (5.3) implies that the image of a proper tricycle through a self-inversion is proper.

Proposition 5.4. Under self-inversion, spinors preserve the integrality.

Proof. Given mutually tangent disks A and B of symbols (see Figure 8)

$$\mathbf{A} = \frac{\dot{x}_A, \dot{y}_A}{A, A^*} \quad \text{and} \quad \mathbf{B} = \frac{\dot{x}_B, \dot{y}_B}{B, B^*},$$

the self-inversion through A results in disks of symbols

$$\mathbf{A}' = \text{Inv}_A(\mathbf{A}) = \frac{-\dot{x}_A, -\dot{y}_A}{-A} \quad \text{and} \quad \mathbf{B}' = \text{Inv}_A(\mathbf{B}) = \frac{\dot{x}_B + 2\dot{x}_A, \dot{y}_B + 2\dot{y}_A}{B + 2A}.$$

Denoting $u = \text{spin}(A, B)$ and $u' = \text{spin}(B', A')$, the square of the spinor from A to B , understood as a complex number, is

$$u^2 = \begin{vmatrix} A & B \\ \dot{x}_A & \dot{x}_B \end{vmatrix} + i \begin{vmatrix} A & B \\ \dot{y}_A & \dot{y}_B \end{vmatrix} \quad (5.4)$$

while the square of the spinor $\text{spin}(A', B')$ under inversion through ∂A is

$$u'^2 = \begin{vmatrix} -A & B + 2A \\ -\dot{x}_A & \dot{x}_B + 2\dot{x}_A \end{vmatrix} + i \begin{vmatrix} -A & B + 2A \\ -\dot{y}_A & \dot{y}_B + 2\dot{y}_A \end{vmatrix}. \quad (5.5)$$

The determinants in (5.5) are negatives of the determinants of (5.4). Indeed, add the first column twice to the second, and factor out the sign. Thus $u'^2 = -u^2$, or $u' = \pm iu$. If $u = [m, n]$ then under the inversion we get $u' = [m, -n]$ (up to the sign, of course). Thus, if u is integral, so is u' . \square

In conclusion, the spin under inversion becomes the conjugated vector, \mathbf{u}^+ :

$$\text{spin}(A', B')^2 = u'^2 = -\text{spin}(A, B)^2.$$

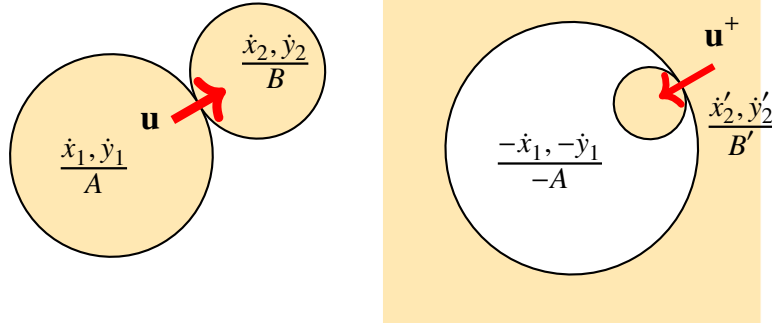


FIGURE 8: Spinor under inversion

5.2. Descartes move of tricycles

Now we inspect the other move of (4.1), which we shall call **Descartes move**. It consists of adding one of the two disks that complete a tricycle to a Descartes configuration and simultaneously removing one of its original three disks. For curvatures,

$$(A, B, C) \rightarrow (A, B, A + B + C \pm 2\sqrt{AB + BC + CA}) \quad (5.6)$$

The move can be done in 6 different ways, hence every tricycle determines a 6-valent graph as its orbit via such moves. The vertices of this graph are all tricycles that appear in a given Apollonian disk packing. It is connected — any two tricycles can be connected by a chain of Descartes moves. A **Descartes walk** is a path in this graph.

Definition 5.5. A **descending Descartes move** is a Descartes move in which the new disk is the greater among the two completing disks, and the removed disk is the one of the greatest curvature.

Remark: If one follows the convention of ordering the curvatures $A \leq B \leq C$, the descending Descartes move corresponds to (5.6). It may be expressed algebraically

$$(A, B, C) \rightarrow (m, \Sigma - M - m, \Sigma - 2\sqrt{AB + BC + CA})$$

where $M = \max(A, B, C)$, $m = \min(A, B, C)$, and $\Sigma = A + B + C$.

Here is an example of two Descartes descending moves

$$(2, 3, 23) \rightarrow (2, 3, 6) \rightarrow (-1, 2, 3)$$

Proposition 5.6. The descending Descartes move applied to a bounded tricycle (tricycle with non-negative curvatures) decreases strictly the weight, with a single exception of tricycle $(0, 0, 1)$

Proof. Assume the order of curvatures to be $0 \leq A \leq B \leq C$. We need to find out if the curvature C' of the new disk replacing the smallest disk C is indeed greater than C (has smaller curvature). Here is a chain of algebraic implications:

$$\begin{aligned} C' &\leq C \\ \Leftrightarrow A + B + C - 2\sqrt{AB + BC + CA} &\leq C \\ \Leftrightarrow A + B &\leq 2\sqrt{AB + BC + CA} \\ \Leftrightarrow 0 &\leq 2AB + 4BC + 4CA - A^2 - B^2 \\ \Leftrightarrow 0 &\leq 3A^2 + 2AB + 3B^2 \end{aligned} \tag{5.7}$$

where in the last expression C is replaced by smaller values, A and B . The last inequality is self-evident, as the right-hand side is a sum of squares: $(A + B)^2 + 2A^2 + 2B^2$. The only situation when the equality $C = C'$ holds is when $A = B = 0$. The primitivity of the triple enforces $C = 1$ resulting in the tricycle $(0, 0, 1)$. \square

Proposition 5.7. The Descartes move preserves the integrality of the disk symbols and of the tangency spinors.

Proof. The integrality of symbols is due to the general rule that the conjugated disks D and D' (two solutions to Descartes formula), satisfy

$$\omega_4 + \omega'_4 = 2\omega_1 + 2\omega_2 + 2\omega_3$$

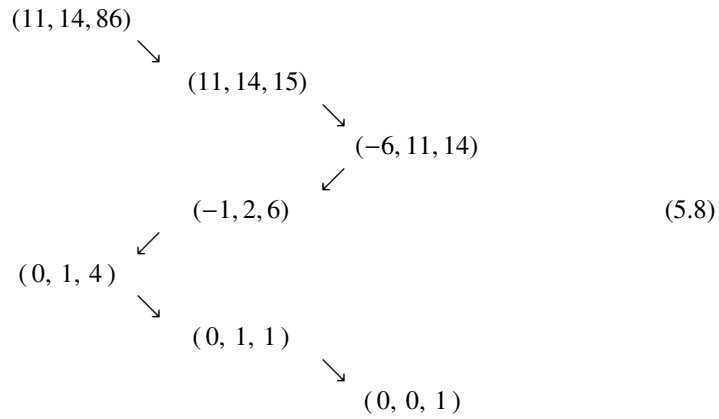
for ω denoting collectively any of the coefficients, \dot{x} , or \dot{y} , or curvature, or co-curvature, of the i -th disk. Since a proper integral tricycle determines a super-integral Apollonian packing, and since the Descartes move travels along tricycles in such a packing, super-integrality is preserved trivially. Since the integrality of two adjacent spinors in any Descartes configuration determines integrality of all its spinors [10], the claim hold trivially. \square

Remark: The Descartes descending move is the critical notion in setting a dynamical system that leads to the definition of the Apollonian depth function in [6, 9].

5.3. Descending process

The process may be alternating between unbounded triples (the greatest circle bounds a disk of negative curvature) and bounded (all three are of positive curvatures). The weight in the descending process is strictly decreasing until reaching the value $w = 1$.

Example: Here is an example of a proper tricycle $(11, 14, 86)$ from Figure 2 undergoing a series of descending moves:



The above chain is to be read from the top down. Arrows to the right denote Descartes moves, to the left — self-inversions.

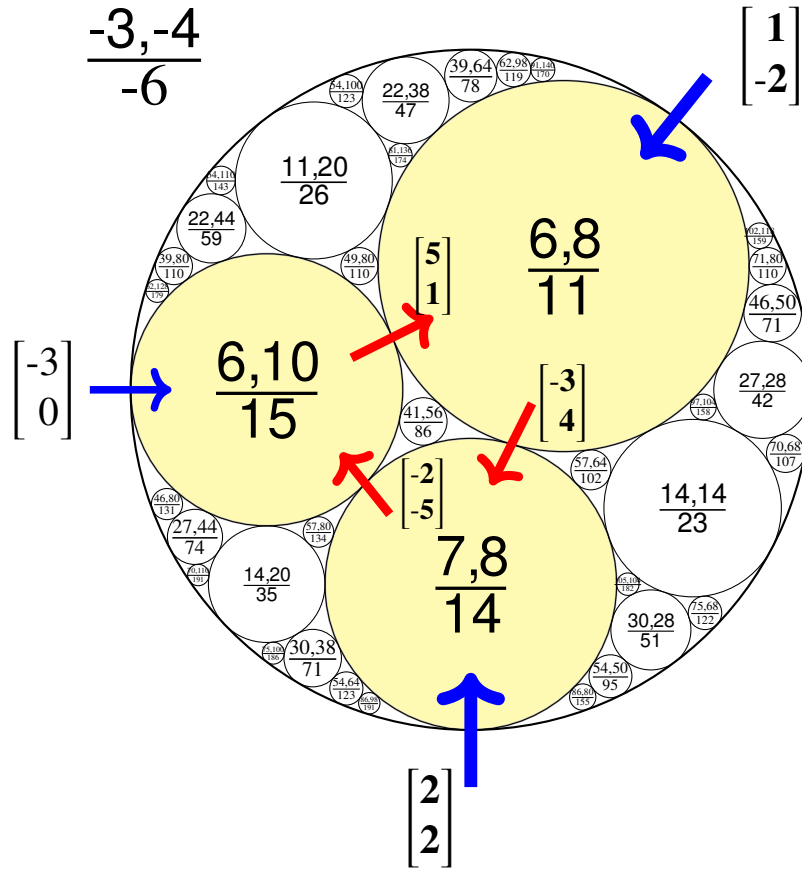


FIGURE 9: All data reconstructed for the triple (11, 14, 15) from Figure 2

The existential aim of the proof aside, the process may be used to actual construction of the “hyper-integral” version of any integral Apollonian disk packing. The result of the reconstruction for the example shown in (5.8) is shown in Figure 9. For practical purposes, one must apply a labeling system to code to perform appropriate “inverses”.

6. The principal triples under descending transformations

Every integral Apollonian packing has a triple of maximal size disks, and the corresponding triple of the minimal curvatures. We shall call them **principal tricycles** and **principal triples**, respectively. Since such a triple determines the Apollonian packing, it may be viewed as its label.

Now, using the concept of the descending transformation, we may construct a graph of descending paths for each of the principal triples. Figure 10 shows the result that includes triples with the negative curvature up to (-12). (A longer list of principal triples may be extracted from the list of Descartes quadruples in [5] or produced with the algorithm discussed there.) In the figure, the principal tricycles are in rectangles, the other in ovals. From any starting tricycle, by descending moves one arrives in configuration (0, 0, 1) where the paths meet. Note that many paths go

through the other principal triples. The branches will be called “threads.”

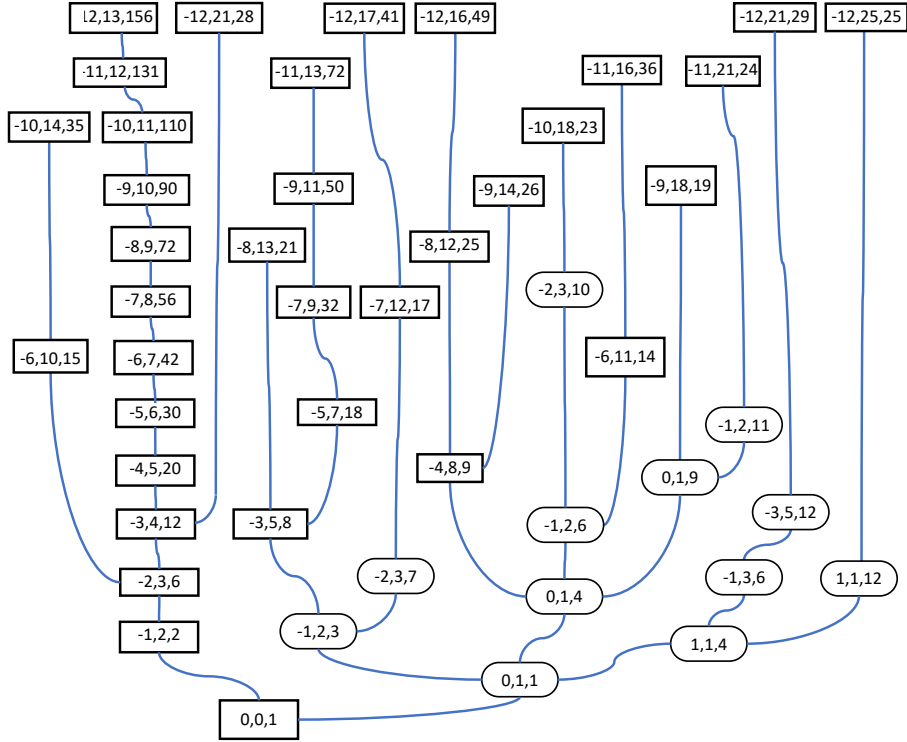


FIGURE 10: Directed graph of primitive defining tricycles

An elementary inspection reveals that most of the paths form polynomial sequences. Table 1 shows the polynomials for the paths in Figure 10.

There is however one surprise. One of the paths is not polynomial but instead consists of triples from the Fibonacci sequence. Note the negative the greatest polynomials are of degree 1, while the third is quadratic. We use the following convention for labeling the Fibonacci sequence:

$$F_0 = 0, \quad F_1 = 1, \quad F_{n+1} = F_n + F_{n-1}$$

Proposition 6.1. Every triple of the consecutive Fibonacci terms, starting with an even-labeled entry (made negative),

$$(-F_{2n}, F_{2n+1}, F_{2n+2}), \quad n > 1$$

defines a principal triple of an Apollonian packing. Moreover, the descending map (self-inversion) carries it to another triple of this kind:

$$(-F_{2n}, F_{2n+1}, F_{2n+2}) \mapsto (-F_{2n-2}, F_{2n-1}, F_{2n}). \quad (6.1)$$

Proof. First, let us see that the triple is proper, that is, it completes to an integral Descartes configuration. Using (3.6), the fourth disk curvature is

$$D = -F_{2n} + F_{2n+1} + F_{2n} \pm 2\sqrt{-F_{2n}F_{2n+1} + F_{2n+1}F_{2n+2} - F_{2n+2}F_{2n}}$$

Label	Example	Formula	Fourth disk
A	$(-12, 13, 156)$	$(-n, n+1, n(n+1))$	n^2+n+1
B	$(-11, 13, 72)$	$(-(2n-1), 2n+1, 2n^2)$	$2n^2 + 2 \pm 2$
C	$(-12, 17, 41)$	$(-(5n-3), 5n+2, 5n^2-n-1)$	$5n^2n+4 \pm 2$
D	$(-12, 16, 49)$	$(-4n, 4n+4, (2n+1)^2)$	$(2n+1)^2+4 \pm 4$
E	$(-11, 16, 36)$	$(-(5n-4), 5n+1, (5n-3)n)$	$5n^2 - n + 5 \pm 4$
F	Fibonacci	$(-F_{2n}, F_{2n+1}, F_{2n+2})$	$2F_{2n+1} \pm 2$
G	$(-10, 14, 35)$	$(-(4n-2), 4n+2, 4n^2-1)$	$4n^2 + 3$

TABLE 1: The formulas for selected threads in the graph in Figure 10.

It takes only the basic identities to arrive at

$$D = 2F_{2n+1} \pm 2,$$

which is evidently integral. The claim of lowering the weight (6.1) is equally simple. \square

Hence, one may define the following chain of Fibonacci tricycles:

$$(0, 1, 1) \mapsto (-1, 2, 3) \mapsto (-3, 5, 8) \mapsto (-8, 13, 21) \mapsto \dots \quad (6.2)$$

This thread is **exceptional** in two ways: (1) unlike the other threads, it is not polynomial; (2) the proportions of the tricycles do not collapse to $(-1, 1, 0)$ with the increasing n , while the others do. To clarify the second property, consider the thread denoted D. The ratios of the second and the third disk to the first become in the limit:

$$\lim_{n \rightarrow \infty} \frac{4n}{4n+4} = 1, \quad \lim_{n \rightarrow \infty} \frac{4n}{(2n+1)^2} = 0,$$

which means the greater of the two disks inside is approaching the external disk, while the smaller disappears to a point. The same concerns the other polynomial threads shown in Figure 10.

In contrast, the triples of the ‘‘Fibonacci thread’’ (6.2), the proportions approach the shape known in Ancient Greece as an ‘‘arbelos’’ with a particular split of the diameter, namely the golden cut. It is shown in Figure 11, left, and the Pappus chains on the right side.

$$\frac{1}{\varphi} + \frac{1}{\varphi^2} = 1$$

Remark: Every disk in the ‘‘golden arbelos’’ has curvature of the form $m\varphi + n$ for some integers $m, n \in \mathbb{Z}$ as assured that the first four are such. In particular, the curvatures of the Pappus chain made by disks passing through the left disk φ and going to the right and to the left are as follows:

$$\begin{aligned} (n^2 + 1)\varphi : & \quad \varphi^2 = \varphi, 2\varphi, 5\varphi, 10\varphi, 17\varphi, \dots \\ (n^2 + 1)\varphi - (n^2 - 1) = \varphi^2 + \frac{n^2}{\varphi} : & \quad \varphi^2 = \varphi + 1, 2\varphi, 5\varphi - 3, 10\varphi - 8, \dots \end{aligned}$$

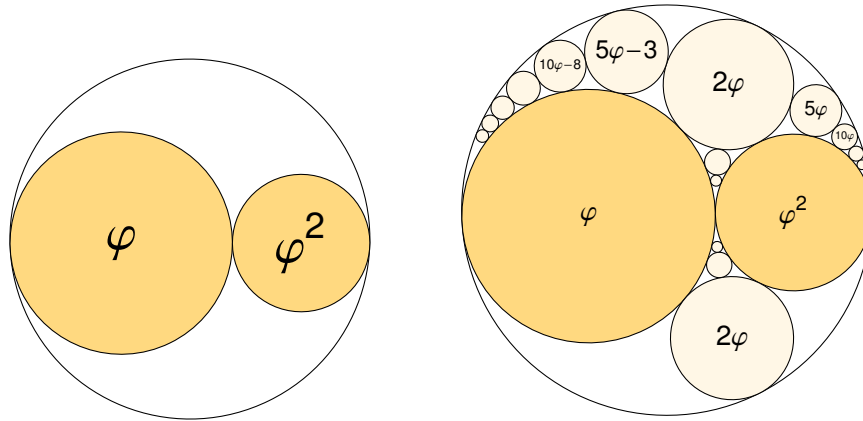


FIGURE 11: Golden arbelos and its Pappus chains

We suggest extending the term “Pappus chain” to any chain of disks that is squeezed between two tangent disks. The Pappus chain squeezed between the disks φ and φ^2 is:

$$2n^2\varphi + n^2 - 1 : \quad -1, 2\varphi, 8\varphi + 3, 18\varphi + 8, \dots$$

And clearly, for $n = 0$ we get (-1) , the greatest enclosing disk.

Performing the reversed descending of the Fibonacci thread will produce a system of tricycles shown in Figure 12. The points of tangency of the circles are

$$P_n = \frac{F_{n-1}^2, 2F_n^2}{F_{2n+1}}$$

They all lie on a single circle $\frac{-1,1}{1}$ and have a point limit:

$$P = \lim_{n \rightarrow \infty} P_n = \left(\frac{5 + 2\sqrt{5}}{5}, \frac{5 - \sqrt{5}}{5} \right)$$

The position of the point is interesting: Points $(-1, 0)$ (P_x), P , $(-1, P_y)$ form a golden rectangle, the one of sides in the golden proportion. The other rectangle that includes points $(-1, -1), (0, 1), P$, is in the proportion 1:2. This “Fibonacci circle” is interesting on its own and will be presented in a subsequent note.

Whether there exist other exceptional threads is an interesting question.

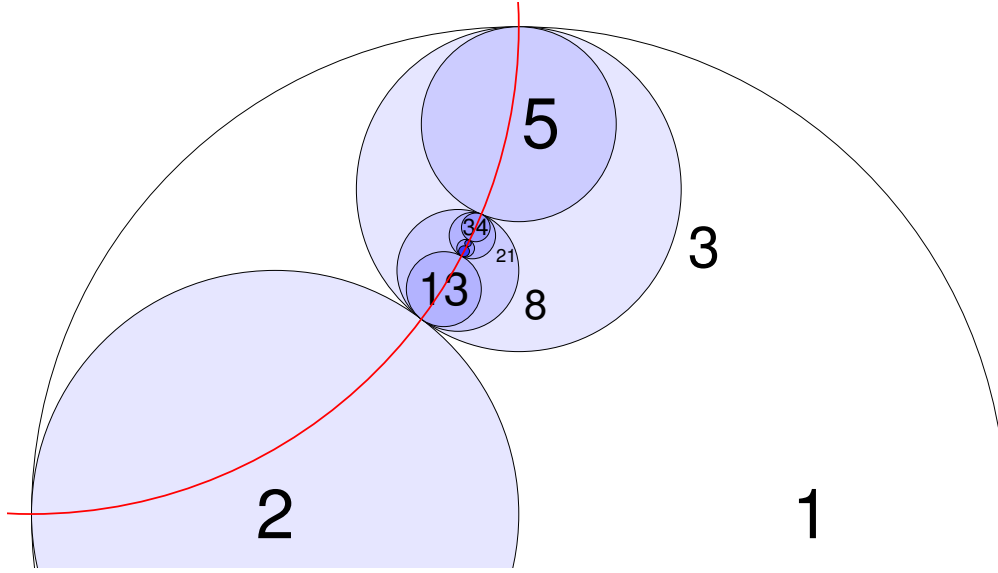


FIGURE 12: The chain of the Fibonacci thread, realized in the plane.

7. The group-theoretic aspect

In this section we rewrite the story with the group-theoretic context clarified.

First, one needs to distinguish between the tricycles as the actual geometric triads of disks located in \mathbb{R}^2 , and the triples of numbers representing their curvatures that can be treated algebraically. We start with the latter. Equip \mathbb{R}^3 with inner product defined by matrix

$$G = \frac{1}{2} \begin{bmatrix} 0 & 1 & 1 \\ 1 & 0 & 1 \\ 1 & 1 & 0 \end{bmatrix} \tag{7.1}$$

In explicit notation, the quadratic form is:

$$Q(\mathbf{v}) \equiv |\mathbf{v}|^2 = xy + yz + zx \quad \text{for } \mathbf{v} = [x, y, z]^T$$

The space (\mathbb{R}^3, G) is isomorphic to a two-dimensional Minkowski space $\mathbb{R}^{1,2}$ of signature $(+, -, -)$, as can be demonstrated with $4Q = (x + 2y + z)^2 - (x - z)^2 - (2y)^2$. Define the subset of triples of integers:

$$\mathcal{T} = \left\{ \mathbf{v} \in \mathbb{Z}^3 : |\mathbf{v}| \in \mathbb{N}, w(\mathbf{v}) > 0, \gcd(v) = 1 \right\} \subset \mathbb{Z}^3$$

where \mathbb{N} includes zero. The three restrictions are repeated here explicitly

- (i) $w(\mathbf{v}) = a + b + c > 0$
- (ii) $|\mathbf{v}| \equiv \sqrt{ab + bc + ca} \in \mathbb{N} = \{0, 1, 2, \dots\}$
- (iii) $\gcd(\mathbf{v}) \equiv \gcd(a, b, c) = 1$

These conditions imply that such triples can be realized as curvatures of disks in tricycles. In particular, that at most one number can be negative and its absolute value smaller than any of the two remaining, and that tricycle is proper, i.e., it may

be completed to an integral Descartes quadruple due to (ii). One may think of them as tricycles with unassigned position or orientation in the Euclidean plane \mathbb{R}^2 .

There are two groups acting in this space:

$$\begin{aligned} \text{APO}^*(3) &= \text{the group generated by Descartes moves} \\ \text{KAL}(3) &= \text{the group generated by self-inversions} \end{aligned}$$

The group generated by the union of generators of both groups will be called the **Descartes tricycle group** and this fact will be denoted with the symbol “ $\dot{\cup}$ ”:

$$\text{DES}^*(3) = \text{APO}^*(3) \dot{\cup} \text{KAL}(3)$$

It acts transitively on the set \mathcal{T} , which is the main point of Proposition 4.1. The notation and terminology in a wider context is addressed in the Appendix. A short description of both groups follows.

1. The **kaleidoscope group** $\text{KAL}(3)$ generated by **self-inversions** represented by linear transformations given by the following matrices:

$$M_1 = \begin{bmatrix} -1 & 0 & 0 \\ 2 & 1 & 0 \\ 2 & 0 & 1 \end{bmatrix}, \quad M_2 = \begin{bmatrix} 1 & 2 & 0 \\ 0 & -1 & 0 \\ 0 & 2 & 1 \end{bmatrix}, \quad M_3 = \begin{bmatrix} 1 & 0 & 2 \\ 0 & 1 & 2 \\ 0 & 0 & -1 \end{bmatrix}. \quad (7.2)$$

The generators satisfy $M_1^2 = M_2^2 = M_3^2 = I$ (identity matrix) and preserve the inner product (7.1):

$$M_i^T G M_i = G \quad \forall i = 1, 2, 3.$$

thus, they generate a discrete subgroup of the Lorentz group

$$\text{KAL}(3) = \text{gen} \{M_1, M_2, M_3\} \subset \text{O}(G, \mathbb{Z}) \cong \text{O}_{(1,2)}(\mathbb{Z})$$

2. The **nonlinear Apollonian group** generated by **tricycle Descartes moves** $\text{APO}^*(3)$ represented by 6 generators:

$$\text{APO}^*(3) = \text{gen} \{N_{1\pm}, N_{2\pm}, N_{3\pm}\}$$

where

$$\begin{aligned} N_{1\pm}(a, b, c) &= (w(\mathbf{v}) \pm 2|\mathbf{v}|, b, c), \\ N_{2\pm}(a, b, c) &= (a, w(\mathbf{v}) \pm 2|\mathbf{v}|, c), \\ N_{3\pm}(a, b, c) &= (a, b, w(\mathbf{v}) \pm 2|\mathbf{v}|) \end{aligned} \quad (7.3)$$

The group preserves the set \mathcal{T} , and transfers tricycles in a transitive way to other tricycles in the same Apollonian packing, hence the adjective “Apollonian” in the name. The star is to indicate that it is nonlinear and is not equivalent to the well-known Apollonian group of [2].

Graph structure. The Cayley graph of the groups are presented in Figure 13. The groups impose a similar structure on the set of tricycles \mathcal{T} , which may be viewed as a graph with tricycles as vertices, and the edges defined by the group action:

Type 1: There exists an edge (a, b) if $b = M_i a$ for some M_i .

Type 2: There exists an edge (a, b) if $b = N_i a$ for some N_i .

The type 1 subgraph is three-valent and forms an infinite tree shown in Figure 13, left. Such a graph is known as $z = 3$ Bethe lattice. Type 2 subgraph is 6-valent and is not cycle-free. (But it may be viewed as a cycle-free infinite ensemble of tetrahedrons joined at their vertices.) Every regular point of \mathcal{T} is thus a 9-valent vertex, with six edges going along the fiber, and three across the fiber bundle. The edges may be oriented by the weight function:

$$a \rightarrow b \quad \text{if} \quad w(b) < w(a).$$

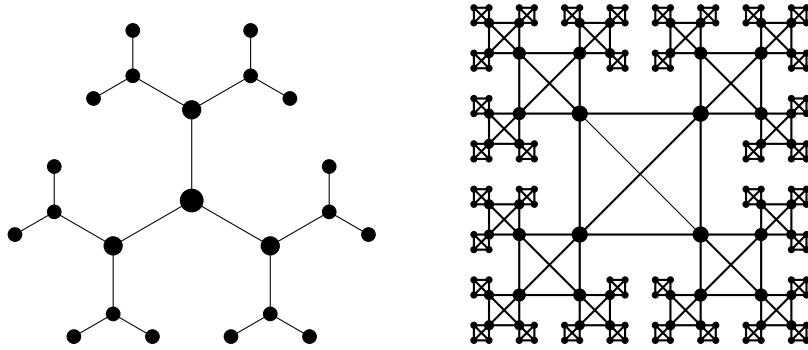


FIGURE 13: Discrete structure of the groups. Left: generated by the three self-inversions; Right: generated by the six Descartes moves. It also reflects the local structures of \mathcal{T} as a graph. Left: along fibers, right: across fibers.

The fiber geometry of the space of tricycles. The action of the group of Descartes moves turns \mathcal{T} into a fiber bundle with the natural projection

$$\pi_{\mathcal{A}} : \mathcal{T} \rightarrow \mathcal{T}/\text{KAL}(3) \cong \mathcal{A} \tag{7.4}$$

where the factor space

$$\mathcal{A} = \mathcal{T}/\text{APO}^*(3) \cong \{\text{all integral Apollonian packings}\}$$

can be identified with the set of the integral irreducible Apollonian disk packings, and the fibers are the group orbits. Each fiber contains all triples in the particular Apollonian packing. Thus, for a given tricycle t , the set

$$\pi^{-1} \circ \pi(t) \cong \text{APO}^*(3) \cdot t$$

consists of all triples in the Apollonian packing that contains t (with no particular location in \mathbb{R}^2 , of course).

Every fiber has a weight-minimal element coinciding with the principal tricycle of the corresponding Apollonian packing. Note that starting with an arbitrary vertex in the fiber and moving down the weight is what defines the “depth function” discussed in [6, 9].

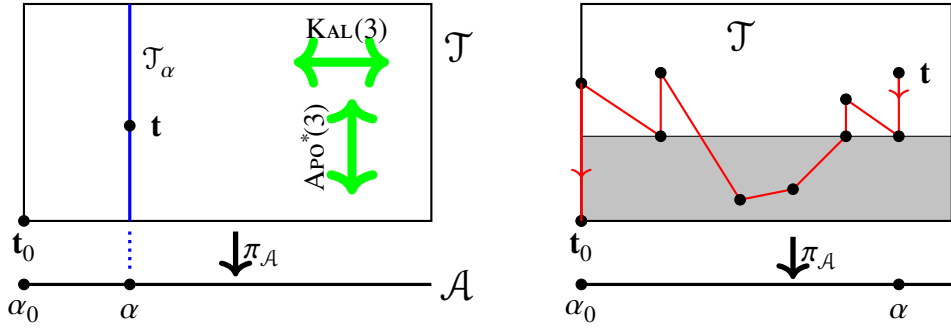


FIGURE 14: Left: The space of triples as a fiber bundle. Apollonian belt is denoted α_0 . Right: A weight-descending path.

Figure 14, left, shows the fiber bundle structure (7.4). The groups are acting “vertically” and “horizontally”. That is, elements of $\text{KAL}(3)$ permute the elements of the fibers but do not permute fibers

$$\pi_A \circ \text{KAL}(3) = \pi_A$$

while the action of $\text{KAL}(3)$ does not preserve the fiber structure, i.e., in general, non-identity elements $g \in \text{KAL}(3)(2)$ skater element of a fiber to different fibers, i.e. in general

$$\pi_A(t) \neq \pi_A(g(t))$$

with exception when $\mathbf{t} \in \pi_A^{-1}(\alpha_0)$ contains a 0. Group $\text{APO}^*(3)$ acts transitively on on each fiber, and group $\text{DES}^*(3) = \text{APO}^*(3) \cup \text{KAL}(3)$ acts transitively on \mathcal{T} .

Geometric meaning of the inner product. The inner product (7.1) has a clear geometric meaning. As is well known, for a given three disks of curvatures a, b, c , the curvature of the circle K going through the points of tangency is $\sqrt{ab + bc + ca}$, which coincides with $|\mathbf{v}|$, where $\mathbf{v} = [a, b, c]^T$. The preservation of the inner product by the self-inversions is beautifully illustrated by the fact that the circle K is preserved by these transformations. Figure 15, left, shows tricycle of disks with curvatures 11, 14, 15, and the inversions of the last two through “11”, assuming curvatures 36 and 37. The limit of the iteration of self-inversions of the original disks is the circle K ; see the right side of the figure.

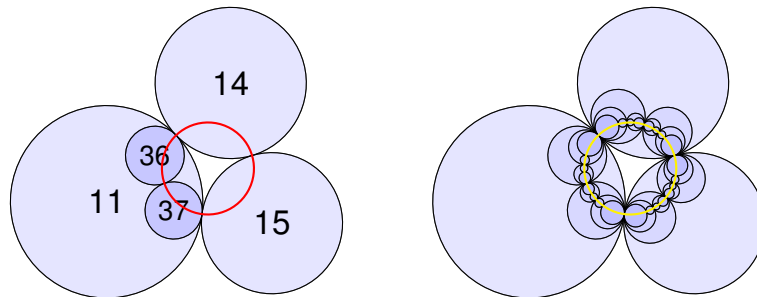


FIGURE 15: The limit set of the action of the tricycle group.

Geometrization of the triples. Now to produce the hyper-integral Apollonian packing in the Euclidean plane given an integral packing devoid of any information o locations, we need another fiber bundle. Let \mathcal{T}_{geo} represent the set of (integral proper) tricycles located in \mathbb{R}^2 . Among others, it contains the tricycle denoted $\bar{\mathbf{t}}_0$ visualized in Figure 4. There is a group of Euclidean motions $E(2)$ (group of isometries, generated by rotations, translations, and reflections) acting on this set. The group action turns the set into a fiber bundle over $\mathcal{T} \cong \mathcal{T}_G/E(2)$, with projection

$$\pi_{\mathcal{T}} : \mathcal{T}_{\text{geo}} \rightarrow \mathcal{T}$$

There is a natural lift of the action of the groups 1 and 2 to the bundle defined as follows. Elements of \mathcal{T}_{geo} may be identified with matrices

$$t = \begin{bmatrix} \dot{x}_A & \dot{y}_A & A \\ \dot{x}_B & \dot{y}_B & B \\ \dot{x}_C & \dot{y}_C & C \end{bmatrix}$$

In the case of self-inversions, the generators are defined by exactly the same matrices as in (7.2). In this context they will be denoted with over-bars: \bar{M}_1 , \bar{M}_2 , and \bar{M}_3 , respectively. In the case of the action of the self-inversion group $\text{KAL}(3)(2)$, the action is defined as

$$\bar{N}_1 : \begin{bmatrix} \dot{x}_A & \dot{y}_A & A \\ \dot{x}_B & \dot{y}_B & B \\ \dot{x}_C & \dot{y}_C & C \end{bmatrix} \rightarrow \begin{bmatrix} f(\dot{x}_A, \dot{x}_B, \dot{x}_C) & f(\dot{y}_A, \dot{y}_B, \dot{y}_C) & g(A, B, C) \\ \dot{x}_B & \dot{y}_B & B \\ \dot{x}_C & \dot{y}_C & C \end{bmatrix}$$

where

$$g_{\pm}(\mathbf{v}) = w(\mathbf{v}) \pm 2\sqrt{Q(\mathbf{v})} \quad \text{and} \quad f_{\pm}(\mathbf{v}) = w(\mathbf{v}) \pm 2\sqrt{Q(\mathbf{v}) + 1}$$

or, explicitly,

$$\begin{aligned} f_{\pm}(x, y, z) &= x + y + z \pm 2\sqrt{xy + yz + zx + 1} \\ g_{\pm}(x, y, z) &= x + y + z \pm 2\sqrt{xy + yz + zx} \end{aligned}$$

The other generators are defined analogously.

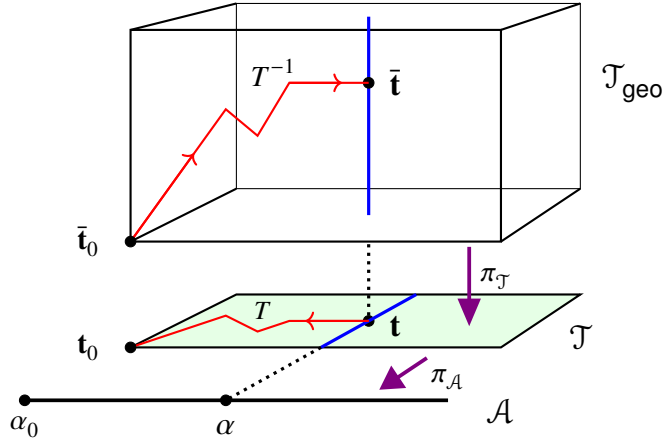


FIGURE 16: The space of geometric tricycles as a fiber bundle. Point t represents the starting triple, t_0 — the base triple $(0, 0, 1)$, \bar{t}_0 — the base tricycle in the hyper-integral location, T denotes the transformation that brings t to t_0 , T^{-1} its inverse applied to \bar{t}_0 and bringing it to the hyper-integral location \bar{t}

Descending and ascending path. On the right side of Figure 14, the darker region symbolizes the unbounded number triples, i.e. containing negative or zero entries. The polygonal path that starts at arbitrary tricycle t (that can be selected from some Apollonian packing α) illustrates the process described in Section 4. At every step, if the tricycle is regular (contain no negative curvature disk), apply Descartes move (this moves the triple along the fiber $\pi^{-1}(\alpha)$). Repeat until the first triple with a negative entry is hit. In such a case apply the self-inversion. Repeat the steps until the base triple $\mathbf{t}_0 = (0, 0, 1)$ is reached. The process creates an element $T \in \text{Des}^*(3)$ such that $T(\mathbf{t}) = \mathbf{t}_0$. Apply its inverse to the geometrized version of the base tricycle to get $\bar{\mathbf{t}} = T^{-1}(\bar{\mathbf{t}}_0)$, which is a tricycle with assigned hyperintegral location in the plane, which may be completed to the corresponding Apollonian packing.

8. Proof done with quadruples and Descartes group

The hyper-integrality proof of the previous sections was based on tricycles, the “primitive atoms” of Apollonian packings. But the story may easily be reformulated in terms of Descartes configurations, the “molecules” of the Apollonian packings, which are more familiar in the context of the Apollonian packings. Below we provide such a formulation in a succinct way. As an interesting results, a symmetry group with linear representation, containing the well-known Apollonian group, emerges.

• **Algebra: integral quadruples.** Let $\mathcal{D} \subset \mathbb{Z}^4$ denote the subset of integer quadruplets, written usually as $\mathbf{v} = (a, b, c, d)$ or alternatively as the column vector $\mathbf{v} = [a \ b \ c \ d]^T$, defined by

$$\mathcal{D} = \{ \mathbf{v} \in \mathbb{Z}^4 : \gcd(\mathbf{v}) = 1, Q(\mathbf{v}) = 0, w(\mathbf{v}) > 1 \} \quad (8.1)$$

where

- (i) $\gcd(\mathbf{v}) = \gcd(A, B, C, D)$
- (ii) $Q(\mathbf{v}) = (A+B+C+D)^2 - 2(A^2+B^2+C^2+D^2)$
- (iii) $w(\mathbf{v}) = a + b + c + d$ denotes the weight

The quadratic form Q of (ii) corresponds to Gram matrix

$$G = \begin{bmatrix} -1 & 1 & 1 & 1 \\ 1 & -1 & 1 & 1 \\ 1 & 1 & -1 & 1 \\ 1 & 1 & 1 & -1 \end{bmatrix}, \quad (8.2)$$

which defines an inner product in \mathbb{R}^4 . Notation $Q(\mathbf{v}) = \|\mathbf{v}\|^2 = \mathbf{v}^T G \mathbf{v}$ may also be used. The conditions (i)–(ii) are to capture only primitive quadruplets that can be realized as curvatures of disks in contact. In particular, the second condition is equivalent to the Descartes formula. The last condition excludes the “non-geometric” examples like $(1, -2, -2, -3)$, which satisfy Descartes formula but are not “geometric”. The lowest weight is assumed by $\mathbf{t}_0 = (0, 0, 1, 1)$ up to the permutation of the entries, the “base quadruple.”

Remark: The G turns \mathbb{R}^4 into a Minkowski space of signature $(+, -, -, -)$, which is dual to that discussed in [3]. The condition $Q = 0$ makes the vectors of \mathcal{D} isotropic.

• **Geometry: Descartes configurations.** By \mathcal{D}_{geo} , we denote geometric instances of the quadruples of \mathcal{D} , i.e., the set of concrete Descartes configurations in the plane with explicit position. The elements of \mathcal{D} may be described by matrices

$$\mathbf{q} = \begin{bmatrix} \dot{x}_A & \dot{y}_A & A & A^c \\ \dot{x}_B & \dot{y}_B & B & B^c \\ \dot{x}_C & \dot{y}_C & C & C^c \\ \dot{x}_D & \dot{y}_D & D & D^c \end{bmatrix} \quad \begin{img alt="Diagram of four yellow circles in contact, representing a Descartes configuration." data-bbox="545 828 600 865"/> \quad (8.3)$$

where \dot{x}, \dot{y} are the reduced coordinates, and the third and the last column contain curvatures and co-curvatures, respectively. In a sense, it is vector \mathbf{v} of (8.1) “extended”

to a matrix. We have a natural fibration

$$\pi_{\mathcal{D}} : \mathcal{D}_{\text{geo}} \rightarrow \mathcal{D} : \begin{bmatrix} x_A & y_A & A & A^c \\ x_B & y_B & B & B^c \\ x_C & y_C & C & C^c \\ x_D & y_D & D & D^c \end{bmatrix} \mapsto \begin{bmatrix} A \\ B \\ C \\ D \end{bmatrix}$$

with the group action by the group $E(2)$ of Euclidean motions (rotations and translations and reflections). The fibers (8.3) are the orbits of the group. Each fiber is the full set of all possible locations of a given quadruple in the Euclidean plane.

• **Symmetry groups** in \mathcal{D} and \mathcal{D}_{geo} . The space described above is invariant under the action of a group that we shall call **Descartes group**,

$$\text{DES}(4) = \text{APO}(4) \dot{\cup} \text{KAL}(4)$$

defined by eight generators that may be split into two quadruplets each defining a subgroup, as described below. (In this context, they will be referred to as “small Descartes groups”.) The groups, interestingly, are now linear (hence the lack of the star in the symbol).

(1) The **Apollonian group** $\text{APO}(4)$ is generated by **Descartes moves**, represented by four matrices:

$$M_1 = \begin{bmatrix} -1 & 2 & 2 & 2 \\ 0 & 1 & 0 & 0 \\ 0 & 0 & 1 & 0 \\ 0 & 0 & 0 & 1 \end{bmatrix} \quad M_2 = \begin{bmatrix} 1 & 0 & 0 & 0 \\ 2 & -1 & 2 & 2 \\ 0 & 1 & 1 & 0 \\ 0 & 0 & 0 & 1 \end{bmatrix} \quad M_3 = \begin{bmatrix} 1 & 0 & 0 & 0 \\ 0 & 1 & 0 & 0 \\ 2 & 2 & -1 & 2 \\ 0 & 0 & 0 & 1 \end{bmatrix} \quad M_4 = \begin{bmatrix} 1 & 0 & 0 & 0 \\ 0 & 1 & 0 & 0 \\ 0 & 0 & 1 & 0 \\ 2 & 2 & 2 & -1 \end{bmatrix} \quad (8.4)$$

Each represents a replacement of one of the disk by its conjugation via the remaining three (see (3.6) in Section 3). It has natural representation of acting on the quadruplets of numbers in \mathcal{D} or as geometric transformations of the actual disk arrangements in the Euclidean plane. (Note that it is not equivalent to the tricycle Apollonian group $\text{APO}^*(3)$ in the previews section.) The matrices are known as the means of reconstructing all disks in the Apollonian packing from a given Descartes configuration, and the name “Apollonian group” is already standard [2].

(2) The **kaleidoscope group** $\text{KAL}(4)$ generated by **self-inversions** that are now represented by four matrices

$$N_1 = \begin{bmatrix} -1 & 0 & 0 & 0 \\ 2 & 1 & 0 & 0 \\ 2 & 0 & 1 & 0 \\ 2 & 0 & 0 & 1 \end{bmatrix} \quad N_2 = \begin{bmatrix} 1 & 2 & 0 & 0 \\ 0 & -1 & 0 & 0 \\ 0 & 2 & 1 & 0 \\ 0 & 2 & 0 & 1 \end{bmatrix} \quad N_3 = \begin{bmatrix} 1 & 0 & 2 & 0 \\ 0 & 1 & 2 & 0 \\ 0 & 0 & -1 & 0 \\ 0 & 0 & 2 & 1 \end{bmatrix} \quad N_4 = \begin{bmatrix} 1 & 0 & 0 & 2 \\ 0 & 1 & 0 & 2 \\ 0 & 0 & 1 & 2 \\ 0 & 0 & 0 & -1 \end{bmatrix} \quad (8.5)$$

The matrices represent self-inversions defined in Section 5.1, now extended from triples to Descartes configurations. They can be viewed as acting on vector $v \in \mathcal{D}$, i.e., on quadruples of numbers (algebra), or on the actual quadruples of disks in the Euclidean plane. Interestingly, the matrices of the second group are transposes of the matrices of the first group despite the different geometric origin and interpretation.

Corollary 8.1. The Descartes group preserves integrality of symbols and spinors.

• **Proof of hyper-integrality.** Now we define the transformation that does the trick.

Definition 8.2. The **descending** transformation of Descartes quadruples is the map $T : \mathcal{D} \rightarrow \mathcal{D}$ defined

$$T(\mathbf{v}) = \begin{cases} M_i \mathbf{v} & \text{if } \min(\mathbf{v}) \geq 0 \text{ and } \max(\mathbf{v}) = v_i & \text{(descending Descartes move)} \\ N_i \mathbf{v} & \text{if } \min(\mathbf{v}) = v_i < 0 & \text{(descending self-inversion)} \end{cases} \quad (8.6)$$

In words: if the quadruple has a negative term, perform self-inversion with respect to it. Otherwise, apply the Descartes move with respect to the greatest term.

Proposition 8.3. The descending transformation decreases strictly the weight

$$w(T\mathbf{q}) < w(\mathbf{q})$$

exception for $\mathbf{q}_0 = (0, 0, 1, 1)$ and its permutations, in which case $w(T(\mathbf{q}_0)) = w(\mathbf{q}_0) = 2$.

Proof. (1) Let us use the notation $\mathbf{q} = (a, b, c, d)$. In case of descending Descartes move that applies when $d \geq c \geq b \geq a \geq 0$, the solution for the fourth disk for the given a, b, c is one of the two: $d_{\pm} = a+b+c \pm \sqrt{ab+bc+ca}$. Clearly $d_- < d_+$ with exception of the base quadruple $\mathbf{q}_0 = (0, 0, 1, 1)$, and the claim follows as d_- replaces d_+ in the move. (2) In the case of descending self-inversion, the argument is analogous to the tricycle version. Say $\mathbf{q} = (-a, b, c, d)$ where all $a, b, c, d \geq 0$.

$$w(T\mathbf{q}) = w(a, b-2a, c-2a, d-2a) = w(\mathbf{q}) - 4a < w(\mathbf{q})$$

(Note that in the case of all four curvatures positive the inequality would fail.) \square

Theorem 8.4. All irreducible integral Descartes configurations as quadruples of \mathcal{D} are hyper-integral, i.e., can be located in the Euclidean plane so that they have integral symbols and integral spinors.

Proof. Starting with a quadruple v , the chain of descending transformations

$$T = T_n T_{n-1} \dots T_2 T_1 \quad T_i \in (\text{the set of eight generators})$$

will bring it to a quadruple $\mathbf{q}_0 = (0, 0, 1, 1)$ (coefficients up to permutation). Since the weight is strictly decreasing, one must arrive at \mathbf{q}_0 . Now, start with the geometric Descartes configuration

$$\bar{\mathbf{q}}_0 = \begin{bmatrix} -1 & 0 & 0 & 2 \\ 1 & 0 & 0 & 2 \\ 0 & 0 & 1 & -1 \\ 0 & 2 & 1 & 3 \end{bmatrix} \quad \begin{array}{c} \text{Diagram of four circles in a square frame, with two circles touching the top and bottom sides, and two circles touching the left and right sides. The circles are arranged in a 2x2 grid, with the top and bottom circles touching each other and the left and right circles touching each other. The top and bottom circles also touch the top and bottom sides of the frame, and the left and right circles touch the left and right sides of the frame. The circles are shaded in light yellow.$$

and apply the inverse operation T^{-1} to the configuration $\bar{\mathbf{t}}_0$ to obtain

$$T^{-1} \bar{\mathbf{q}}_0 = T_1 T_2 \dots T_{n-1} T_n \bar{\mathbf{q}}_0$$

where we took into account that for every elementary element we have $T_i^{-1} = T_i$. Since each elementary T preserves the integrality of the symbols, and the parity of curvatures and co-curvatures, as well as the tangency spinors, the claim holds. \square

• **More on the Descartes group.**

Basic facts:

1. The subgroups $\text{Apo}(4)$ and $\text{KAL}(4)$ are, as abstract entities, isomorphic,

$$\text{Apo}(4) \cong \text{KAL}(4)$$

or rather anti-isomorphic, since $(ab)^T = b^T a^T$. What distinguishes them is the way we define their action on \mathcal{D} and on \mathcal{D}_{geo} .

2. The structure of the spaces: The fibers of $(\mathcal{D}_{\text{geo}}, \pi_{\mathcal{D}}, \mathcal{D})$ look like the Bethe lattice of Figure 17. Every vertex in \mathcal{D}_{geo} has another set of four edges directed to vertices of other fibers. The relation between the groups and fibrations is shown below:

$$\begin{array}{ccccc} \text{E}(2) & & \text{Apo}(4) & & \\ \Downarrow & & \Downarrow & & \\ \mathcal{D}_{\text{geo}} & \xrightarrow{\pi_{\mathcal{D}}} & \mathcal{D} & \xrightarrow{\pi_{\mathcal{A}}} & \mathcal{A} \\ & & \mathbb{R} & & \mathbb{R} \\ & & \mathcal{D}/\text{E}(2) & & \mathcal{D}/\text{Apo}(4) \end{array}$$

where the squiggly arrows \rightsquigarrow mean “a group acts on”. The situation is analogous to that in Figure 14, except \mathcal{T} needs to be replaced by \mathcal{D} .

3. The inner Descartes group acts transitively in the set of all Descartes quadruples (configurations) of a given Apollonian packing. In other words, they preserve the fibers of fibration

$$\pi_{\mathcal{D}} : \mathcal{D} \rightarrow \mathcal{D}/\text{Apo}(4) \cong \mathcal{A}$$

The factor space coincides with the set \mathcal{A} of irreducible Apollonian disk packings. Elements of the group $\text{KAL}(4)$ mix the fibers, but not consistently, i.e. in general

$$\pi_{\mathcal{A}}(\mathbf{q}) \neq \pi_{\mathcal{A}}(g\mathbf{q}) \quad g \in \text{KAL}(4), \quad g \neq \text{id}$$

4. The Descartes group is orthogonal:

$$\text{DES}(4) \subset \text{O}(\mathbb{R}^4, G) \cong \text{O}(1, 3; \mathbb{R})$$

as each element X of the generating set satisfies

$$X^T G X = G, \tag{8.7}$$

and so do their products as well.

5. Each generator is an involution, i.e., satisfies $X^2 = \text{id}$. Geometrically, it represents a reflection in the Minkowski space. The reflection is orthogonal with respect to G . The associated axis \mathbf{A} and the invariant hyperplane \mathbf{A}^\perp is shown here for the first generators:

$$\text{For } M_1: \quad \mathbf{A}_1 = [1, 0, 0, 0], \quad \mathbf{A}_1^\perp = \text{span}([x+y+z, x, y, z] : x, y, z \in \mathbb{R})$$

$$\text{For } N_1: \quad \mathbf{B}_1 = [-1, 1, 1, 1], \quad \mathbf{B}_1^\perp = \text{span}([0, x, y, z] : x, y, z \in \mathbb{R})$$

6. The generators represent orthogonal reflection with respect to the inner product G . They be defined from the corresponding eigenvectors \mathbf{v} with the eigenvalue $\lambda = -1$ (call the “axes”) as follows:

$$M_{\mathbf{v}} = \text{id} - 2 \frac{\mathbf{v} \mathbf{v}^T G}{\mathbf{v}^T G \mathbf{v}}$$

For the matrices M , the axes are $[1, 0, 0, 0]$ and the permutations. For the matrices N the axes are $[-1, 1, 1, 1]$ and the permutations.

7. Note that the only eigenvectors of the generators that are contained in the set \mathcal{D} are

$$[1, 1, 0, 0], [1, 0, 1, 0], [1, 0, 0, 1], [0, 1, 1, 0], [0, 1, 0, 1], [0, 0, 1, 1].$$

with the eigenvalue $\lambda = 1$, which are different versions of the base state \mathbf{q}_0 .

8. The topology of the groups: The Cayley graph of each of the “small Descartes” groups $\text{KAL}(4)$ and $\text{APO}(4)$ is similar to that of the free group of rank 2 (but not equivalent, for we have relations $X^2 = \text{id}$ for the generators). The graph is also known under the name of “ $z = 4$ Bethe lattice”, shown in Figure 17.

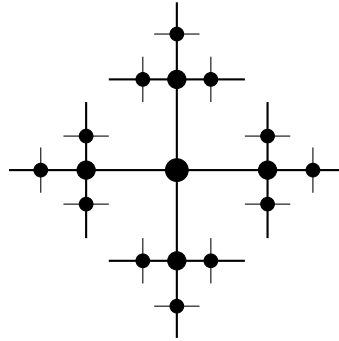


FIGURE 17: Cayley graph of each small Descartes group is an infinite 4-valent cycle-free graph, also known as a $z = 4$ Bethe lattice.

The “big” Descartes group $\text{DES}(4)$ is a graph of valency 8, but it is not cycle-free anymore, since the following identities hold:

$$M_i N_j = N_j M_i \quad \text{whenever } i \neq j$$

or, $[M_i, N_j] = 0$. Hence, e.g., $M_1 N_2 M_1 N_2 = \text{id}$ defines a cycle in the Cayley graph.

9. The intriguing fact that the matrix generators of the two small Descartes groups are transposes of each other can be interpreted with rewriting the orthogonality property (8.7):

$$N_i G M_i = G \quad \text{and} \quad M_i G N_i = G \quad \forall i = 1, 2, 3, 4.$$

10. **Remark:** The fact that the matrices representing the two small groups are transposes of each other is accidental and inherent to the 2-dimensional instance. In 3-dimensional case of 3-disks (balls) in \mathbb{R}^3 , the **kaleidoscope group** $\mathbf{KAL}(5)$ is generated by five matrices analogous to the ones before

$$\begin{bmatrix} -1 & 0 & 0 & 0 & 0 \\ 2 & 1 & 0 & 0 & 0 \\ 2 & 0 & 1 & 0 & 0 \\ 2 & 0 & 0 & 1 & 0 \\ 2 & 0 & 0 & 0 & 1 \end{bmatrix}, \begin{bmatrix} 1 & 2 & 0 & 0 & 0 \\ 0 & -1 & 0 & 0 & 0 \\ 0 & 2 & 1 & 0 & 0 \\ 0 & 2 & 0 & 1 & 0 \\ 0 & 2 & 0 & 0 & 1 \end{bmatrix}, \begin{bmatrix} 1 & 0 & 2 & 0 & 0 \\ 0 & 1 & 2 & 0 & 0 \\ 0 & 0 & -1 & 0 & 0 \\ 0 & 0 & 2 & 1 & 0 \\ 0 & 0 & 2 & 0 & 1 \end{bmatrix}, \dots \text{etc.} \quad (8.8)$$

but the **Apollonian** $\mathbf{APO}(5)$ is generated by five 5×5 matrices:

$$\begin{bmatrix} -1 & 1 & 1 & 1 & 1 \\ 0 & 1 & 0 & 0 & 0 \\ 0 & 0 & 1 & 0 & 0 \\ 0 & 0 & 0 & 1 & 0 \\ 0 & 0 & 0 & 0 & 1 \end{bmatrix}, \begin{bmatrix} 1 & 0 & 0 & 0 & 0 \\ 1 & -1 & 1 & 1 & 1 \\ 0 & 0 & 1 & 0 & 0 \\ 0 & 0 & 0 & 1 & 0 \\ 0 & 0 & 0 & 0 & 1 \end{bmatrix}, \begin{bmatrix} 1 & 0 & 0 & 0 & 0 \\ 0 & 1 & 0 & 0 & 0 \\ 1 & 1 & -1 & 1 & 0 \\ 0 & 0 & 0 & 1 & 0 \\ 0 & 0 & 0 & 0 & 1 \end{bmatrix}, \dots \text{etc.} \quad (8.9)$$

which clearly not mutual transposes.

• Higher dimensions

For the sake of completeness, here is the characterization of the Descartes groups for n -disks in n -dimensional space, represented by $m \times m$ matrices, $m = n + 2$. We use the standard notation where \mathbf{e}_i denotes the column with 1 at the i -th position and zeros everywhere else. Similarly, \mathbf{e}_{ij} is a matrix with 1 at the (ij) -th position and zeros everywhere else.

Consider the pseudo-Euclidean space (\mathbb{R}^m, G) , where the inner product is given by matrix

$$G = \sum_{i=1}^n (3-m) \mathbf{e}_{ii} + \sum_{i \neq j} \mathbf{e}_{ij}.$$

There are three groups generated by $m \times m$ matrices, denoted:

- (1) $\mathbf{APO}(m) = \text{gen} \{ M_i \mid i = 1, \dots, m \}$
- (2) $\mathbf{KAL}(m) = \text{gen} \{ N_i \mid i = 1, \dots, m \}$,
- (3) $\mathbf{DES}(m) = \text{gen} \{ M_i, N_i \mid i = 1, \dots, m \}$

where the matrices are

$$M_i = \text{id} - 2\mathbf{e}_{ii} + \frac{2}{m-3} \sum_{j, j \neq i} \mathbf{e}_{ij}, \quad N_i = \text{id} - 2\mathbf{e}_{ii} + 2 \sum_{j, j \neq i} \mathbf{e}_{ji}.$$

Here are the first matrices of each subgroup:

$$M_1 = \begin{bmatrix} -1 & \frac{2}{m-3} & \dots & \frac{2}{n-1} \\ 0 & 1 & \dots & 0 \\ \vdots & & & \vdots \\ 0 & 0 & \dots & 1 \end{bmatrix} \quad N_1 = \begin{bmatrix} -1 & 0 & \dots & 0 \\ 2 & 1 & \dots & 0 \\ \vdots & & & \vdots \\ 2 & 0 & \dots & 1 \end{bmatrix} \quad (8.10)$$

Basic properties: The matrices are (i) involutions and (ii) orthogonal with respect to G :

$$\begin{aligned} (i) \quad & M_i^2 = N_i^2 = \text{id} \quad \forall i = 1, \dots, n \\ (ii) \quad & X^T G X = G \\ (iii) \quad & \det X = -1 \end{aligned}$$

In general, the generators do not commute, except the case:

$$\text{If } i \neq j \text{ then } [M_i, N_j] = 0$$

The generators are orthogonal reflections in hyperplanes and may be characterized by axes (eigenvectors with eigenvalues $\lambda = -1$):

$$\mathbf{A}_i = \mathbf{e}_i, \quad \mathbf{B}_i = -\mathbf{e}_i + \sum_{j \neq i} \mathbf{e}_j.$$

The generators can be thus defined as:

$$M_i = \text{id} - 2 \frac{\mathbf{A}_i \mathbf{A}_i^T G}{\mathbf{A}_i^T G \mathbf{A}_i}, \quad N_i = \text{id} - 2 \frac{\mathbf{B}_i \mathbf{B}_i^T G}{\mathbf{B}_i^T G \mathbf{B}_i}.$$

Small dimensions: The cases of $m = 4$ and $m = 5$ are given above. The case of $m = 3$ corresponding to 1-disks on a real line is degenerated and only the component $\text{KAL}(3)$ is well-defined. The integrality of the matrices (8.10) breaks for dimensions $m > 5$.

Geometrically, the case $m = 2$ corresponds to the absurd case of the 0-disks in the 0-dimensional space, yet formally it is well-defined; the matrices are:

$$G = \begin{bmatrix} 1 & 1 \\ 1 & 1 \end{bmatrix}, \quad M_1 = \begin{bmatrix} -1 & -2 \\ 0 & 1 \end{bmatrix}, \quad M_2 = \begin{bmatrix} 1 & 0 \\ -2 & -1 \end{bmatrix}, \quad N_1 = \begin{bmatrix} -1 & 0 \\ 2 & 1 \end{bmatrix}, \quad N_2 = \begin{bmatrix} 1 & 2 \\ 0 & -1 \end{bmatrix}.$$

where G is the Gram matrix of the inner product in the space. Note that the first matrix determines the others: $M_2 = -M_1^T$, and the N matrices are the negatives of these two. They produce an interesting subgroup of $\text{SL}^\pm(2)$.

Remark: For additional material see pages at [17].

Acknowledgments

I would like to thank Philip Feinsilver for helpful discussions and his supportive interest in this project.

References

- [1] René Descartes, Oeuvres de Descartes, Correspondence IV, (C. Adam and P. Tannery, Eds.), Paris: Leopold Cerf 1901.
- [2] R. Graham, J. Lagarias, C. Yan, Apollonian circle packings: number theory Journal of Number Theory, 2000
- [3] Jerzy Kocik, A theorem on circle configurations arXiv:0706.0372 (2007, 16 pages).

-
- [4] Jerzy Kocik, Proof of Descartes circle formula and its generalization clarified [arXiv:1910.09174] (2019, 3 pages)
- [5] Jerzy Kocik, On a Diophantine equation that generates all integral Apollonian gaskets, ISRN Geometry.Article ID 348618, 19 pages, 2012. doi:10.5402/2012/348618. [arXiv:2008.04440]
- [6] Jerzy Kocik, Apollonian depth and the accidental fractal, (2020, 35 pages) [arXiv:2002.04135]
- [7] Jerzy Kocik, Clifford algebras and Euclid's parameterization of Pythagorean triples, *Advances in Applied Clifford Algebras (Mathematical Structures)*, **17** 2007 pp. 71-93.
- [8] Jerzy Kocik, Spinors and the Descartes configuration of circles [arXiv:1909.06994] (2019, 21 pages)
- [9] Jerzy Kocik, Apollonian depth, spinors, and the super-Dedekind tessellation [arXiv:2009.02680] (2020, 20 pages)
- [10] Jerzy Kocik, Spinors, lattices, and classification of integral Apollonian disk packings, [arXiv:2001.05866] (2020, 35 pages)
- [11] Jerzy Kocik, Apollonian coronas and a new Zeta function, [arXiv:1909.09941] (2019, 19 pages)
- [12] Jeffrey C. Lagarias, Colin L. Mallows and Allan Wilks, Beyond the Descartes circle theorem, *Amer. Math. Monthly* 109 (2002), 338–361. [eprint: arXiv math.MG/0101066]
- [13] E. Landau, "Über die Einteilung der positiven ganzen Zahlen in vier Klassen nach der Mindestzahl der zu ihrer additiven Zusammensetzung erforderlichen Quadrate." *Arch. Math. Phys.* 13, 305-312, 1908.
- [14] Shanks, D. Non-Hypotenuse Numbers. *Fibonacci Quart.* 13, 319-321, 1975.
- [15] Frideric Soddy, The kiss precise, *Nature*, **137**, page1021(1936)
- [16] Katherine Stange, The sensual Apollonian circle packing, *Expositiones Mathematicae*, **34** 4 (2016), 364-395.
- [17] Apolloniana - a site discussing the geometry of the Apollonian disk packings: [https://apolloniana.blogspot.com/]